DOCUMENT CONTROL SHEET

	ORIGINATOR'S REF.		SECURITY CLASS.
	NLR-TP-2003-228		Unclassified

ORGINATOR
National Aerospace Laboratory NLR, Amsterdam, The Netherlands

TITEL:
Real-time cloud sensing for efficiency improvement of optical high-resolution satellite remote sensing

PRESENTED AT:
IGARSS 2003, Toulouse, France, 21-25 July 2003.

AUTHORS	DATE	PP	REF
T. Algra	May 2003	6	4

DESCRIPTORS
Cloud avoidance scheduling
Cloud cover
Data acquisition
Remote-sensing

ABSTRACT
Cloud sensing provides the ability to point the optical axis of the satellite remote sensing instrument to cloud-free areas on the basis of previously acquired cloud cover information. In this way the effective imaging capacity of the mission can be improved. The cloud cover information may be acquired in real-time for optimal performance. This paper explores a number of real-time cloud sensing concepts. The performance of the different options is assessed by analysis and simulation. It is concluded that the imaging capacity of a high-resolution optical remote sensing satellite can be improved by up to 100%.

Nationaal Lucht- en Ruimtevaartlaboratorium
National Aerospace Laboratory NLR

NLR-TP-2003-228

Real-time cloud sensing for efficiency improvement of optical high-resolution satellite remote sensing

T. Algra

This report is presented at IGARSS, Toulouse, France, 21 - 25 July 2003.

Customer:	National Aerospace Laboratory NLR
Working Plan number:	R.3.A.3
Owner:	National Aerospace Laboratory NLR
Division:	Space
Distribution:	Unlimited
Classification title:	Unclassified
	May 2003

Approved by author:	Approved by project manager:	Approved by project managing department:
16/6	16/6	

Contents

1 Table
1 Figure

List of Symbols

α	Along-track pointing angle (pitch)
β	Cloud sensor look angle
a	Satellite altitude
D	Length of Area of Interest
D_{x1}	Cloud displacement in along-track direction, front side
D_{x2}	Cloud displacement in along-track direction, aft side
D_y	Cloud displacement in cross-track direction
h	Cloud height
IC_{eff}	Average successful images per pass
M	Margin ratio
N	Number of pending requests
N_i	Number of possible images per pass
P	Probability of a cloud-free target
Q(f)	Probability density function of fraction of cloud-free targets
S	Swath width
T_{slew}	Average slew time
v	Satellite speed
w	Cloud speed

Real-time cloud sensing for efficiency improvement of optical high-resolution satellite remote sensing

Theo Algra
National Aerospace Laboratory NLR
The Netherlands
algra@nlr.nl

Abstract—**Cloud sensing provides the ability to point the optical axis of the satellite remote sensing instrument to cloud-free areas on the basis of previously acquired cloud cover information. In this way the effective imaging capacity of the mission can be improved. The cloud cover information may be acquired in real-time for optimal performance. This paper explores a number of real-time cloud sensing concepts. The performance of the different options is assessed by analysis and simulation. It is concluded that the imaging capacity of a high-resolution optical remote sensing satellite can be improved by up to 100%.**

Keywords-remote sensing; cloud cover; data acquisition; cloud avoidance scheduling

I. INTRODUCTION

Cloud cover is a severe problem in optical satellite remote sensing. Depending on the local climate, often a significant part of the recorded images is not acceptable due to cloud contamination. This has a negative impact on the effective imaging capacity of the satellite observation system, i.e. the total surface area successfully imaged per unit of time.

The concept of Cloud Avoidance Scheduling has been applied in the Landsat 7 mission. Recording of cloudy areas is avoided using cloud cover prediction data based on a numerical weather model as an input to the satellite tasking process [1]. Another method is Selective Compression, performed on-board the satellite. This means that imaged cloud contaminated data are discarded and not stored for later downlinking [2]. The two methods improve the efficiency of the use of data storage and communication resources, but do not increase the effective imaging capacity of the optical instrument.

Potentially higher efficiency is obtained if the pointing ability of the optical axis, if available, is used to actively select cloud free areas. The necessary cloud information can be derived from numerical weather models (usually half a day or more in advance), from meteorological satellites (one or more hours in advance), or from a real-time sensor. Such a sensor may be accommodated on the observation satellite itself or on a microsatellite, flying ahead.

The advantages of the real-time cloud sensor approach are:

1. The necessary cloud information is available at every position
2. The delay between cloud cover acquisition and actual observation is small and guarantees accurate cloud cover prediction.
3. The resolution of the cloud sensor can be tuned to the requirements of the observation mission.
4. The method is not dependent of other systems such as meteorological satellites, communication networks, or providers of numerical weather prediction data.

This paper discusses such a real-time cloud avoidance approach, which we named "cloud sensing".

Section II defines a number of possible real-time concepts. The performance gain of real-time cloud sensing is mathematically estimated in Section III, while Section IV presents simulation results based on real high-resolution cloud data followed by concluding remarks in Section V.

This paper is based on research results obtained in the framework of the Euclid RTP9.6 project, which covered Earth observation technical concepts and co-ordination.

II. REAL-TIME CONCEPTS

A. On-board cloud sensor

Assume a typical state-of-the-art very high-resolution (VHR) optical satellite. The sensor can be pointed both in the cross-track and along-track direction by $\pm 45°$and the instantaneous field of view (IFOV) is 10 km. The sensor steering is agile, meaning that the average slew time between two successive image strips is < 10 seconds. The cloud sensor's look angle β should be larger than +45° in the fore direction with a FOV of 70° in the cross-track direction. Obviously, β should be as small as possible in order to limit geometrical distortion of the cloud cover image. However, some delay between the imaging moment of a location by the cloud sensor and the entrance of that same location in the main sensor's field of view is necessary to allow pointing-transitions and cloud information processing. We assume that a maximal total delay of 10 seconds is sufficient.

A complication is that usually the main instrument's pointing is accomplished by tilting the satellite body. Consequently the cloud sensor has to be pointable too, using a two-dimensional gimballing system.

The parallax effect and the motion of clouds due to winds may introduce inaccuracy in the cloud mapping process. Neglecting errors due to inaccurate georeferencing, the geolocation error can be expressed as a function of wind speed w, satellite speed v, altitude a, cloud sensor look angle β, along track pointing angle α (pitch), and cloud height h:

$$D_{x1} = h(tg\beta - tg\alpha) + \frac{(a-h)w_x}{v}(tg\beta - tg\alpha)$$

$$D_{x2} = \frac{(a-h)w_x}{v}(tg\beta - tg\alpha)$$

$$D_y = \frac{(a-h)w_y}{v}(tg\beta - tg\alpha)$$

D_{x1} is the possible cloud displacement in along-track direction on the front side of the target area and D_{x2} at the aft side. D_y is the possible displacement in cross-track direction.
With β = 48° and typical values for a-h (600 km) and v (7 km/s) this reduces to:

$$D_{x1} \approx (h + 86w_x)(1.11 - tg\alpha)$$

$$D_{x2} \approx 86w_x(1.11 - tg\alpha)$$

$$Dy \approx 86w_y(1.11 - tg\alpha)$$

For example a cloud height of 5 km and a wind speed of 50 km/hr result in $D_{x1} \leq 13.07$ km. This is larger than the basic image area (s x s km). Consequently, if w and h are unknown on-board the satellite, the decision whether to image an area should be based on a larger area which includes a margin area. Obviously this reduces the number of cloud free selections and will decrease the efficiency somewhat. The margin ratio is defined as the factor

$$M = \sqrt{\frac{(D_{x1} + D_{x2} + s)(2D_y + s)}{s^2}}$$

For the above-mentioned wind speed and cloud height, M = 1.75, worst case.

B. Cloud sensor on free flying microsat

Another option is to accommodate the cloud sensor on a microsatellite in the same orbit as the observation satellite, flying at a fixed distance ahead. The microsat performs cloud detection and geolocation. A low rate communication link transmits the cloud data to the VHR satellite. We will distinguish three options:

i) Microsat on short distance

The cloud sensor's viewing direction is fixed nadir. The distance between the microsat and the VHR satellite is such that the sensor acquires cloud image data just before the corresponding area enters the field of view of the VHR satellite. In other words the distance is close to a. The parallax error is smaller than in the on-board sensor case due to β = 0. The error due to cloud motion is the same. This results in M = 1.49 for h=5km and w =50 km/hr

ii) Microsat on larger distance

In the above concepts the eventual imaging schedule is automatically generated. However, sometimes it is required that the final schedule is checked and possibly adjusted by an operator. This means that the cloud data has to be downlinked from the microsat, followed by processing, final adjustments, and uplinking to the VHR satellite. In other words a longer distance is required between the two satellites. The extra time needed for this man-in-the-loop process is assumed at least 5 minutes. This corresponds to a distance of about 2100 km between the satellites. Obviously, cloud motion errors will be larger. The margin ratio M becomes 1.76 in this case.

iii) Microsat with dual sensor on larger distance

A modification of the previous concept is the use of a dual cloud sensor with a forward looking and a backward looking part. This allows stereo imaging and estimation of cloud heights as well as cloud speeds. In principle, the parallax and cloud motion errors can be eliminated, resulting in M=1.

Table I lists the main characteristics of the above-mentioned concepts.

III. MATHEMATICAL MODEL

Suppose a square area of interest (AOI) of typically, 500 x 500 km. Assume an unremitting number of N (average) pending target observation requests, all for 10x10 km areas, randomly dispersed over the AOI. Obviously, the successful cloud-free observations during a pass are replaced by new requests for the following pass. Assume an agile spacecraft that can point across-track and along-track ± 45°. This allows

$N_i \approx \frac{2a + D}{s + vT_{slew}}$ images to be taken during one pass.

D is the size of the AOI and T_{slew} is the average time needed to change the instrument pointing from one target to the other.

Let the probability that a target is cloud-free be equal to p, i.e. the cloudiness < cloudiness-threshold (20%, for example). Then, without cloud sensing, on the average, pNi successful images can be taken during one pass. This is the effective imaging capacity IC_{eff} for the particular AOI.

Example: p=0.3, Ni=25, gives IC_{eff} = 0.3Ni = 7.5.

However, in the case of cloud sensing, cloud-free images can be selected from the N pending requests up to a maximum of Ni. We approximate the probability distribution Q(f) of the fraction of cloud-free targets f by the semi-uniform function

$$Q(f) = 11 - 20p \quad for\ f \leq 0.1$$

$$Q(f) = 2\frac{2}{9}p - \frac{1}{9} \quad for\ f > 0.1$$

for p ≤ 0.5. For 0.1N ≤ Ni ≤ N the imaging capacity can be calculated as

$$IC_{eff} = -\frac{c}{2N}N_i^2 + cN_i + 0.05N(1-c) \quad with \quad c = \frac{p - 0.05}{0.45}$$

Example: p=0.3, Ni=25, and N=75, gives IC_{eff} =0.53Ni = 13.24.

For N = 10Ni, considered as a practical maximum, and p ≤ 0.5, the imaging capacity becomes

$$IC_{eff} = (p + 0.45)N_i$$

In other words, cloud sensing improves the effective imaging capacity with a gain of maximally $\frac{p+0.45}{p}$.

Note that the average pending time of a request will be longer than in the non-cloud sensing case, especially for large N. A margin ratio > 1 will decrease p, and hence decrease the cloud sensing gain.

IV. SIMULATIONS

Simulations have been performed based on real cloud cover data. The cloud database is the CHANCES database, which provides global historical cloud cover data with 5 km resolution, and 1 hour temporal resolution [3].

Fig. 1 shows the results of an AOI located in Western Europe, 500 x 500 km, with the centre located at latitude 49.75° and longitude 8.65°. With an average slew time Tslew=8 seconds, Ni amounts 25. The figure shows the average number of successful images per pass, with a cloudiness threshold of 20%, as a function of N and with the margin ratio M as a parameter.

The average value of p was 0.28 in this case. The simulation results show a close similarity with the above-described model. The margin ratio has a clear impact on IC_{eff}.

V. CONCLUDING REMARKS

The effective imaging capacity of a high-resolution satellite can be significantly improved by real-time cloud sensing. Simulations based on real cloud cover data confirm theoretical results.

Of the single sensor concepts, a cloud sensor accommodated on a microsatellite flying ahead of the VHR satellite is the best performing option. The microsat can be launched, piggy backed to the VHR satellite. The improved imaging capacity, especially in frequently clouded areas, will compensate the relative modest investments related to the microsatellite.

Cloud sensing may also be based on information from a meteorological satellite such as MSG for example. Better cloud prediction models using additional weather data might compensate the lower accuracy due to the longer delay. One example of such a model is MetCast [4]. However, such models are only available for limited regions at the moment.

REFERENCES

[1] Gasch, J., K.A. Campana, "Cloud cover avoidance in space-based remote sensing acquisition. In Algorithms for Multispectral, Hyperspectral, and Ultraspectral Imagery IV, Proc. SPIE Vol. 4049, pp. 336-347, 2000

[2] Algra, T., et al, "Cloud sensing and satellite operations", Euclid RTP9.6 Final report, RTP96/01/NLR.TA/213/FR, NLR-CR-2001-316, Amsterdam, 2001

[3] Haar, T.H. Vonder, et al, "Climatological and Historical Analysis of Clouds of Environmental Simulations (CHANCES) Database – Final report. Philips Laboratory, Hanscom Air Force Base, Mass., PL-TR-95-2101, 71 pp. (limited distr.), 1995

[4] Linden, N. van der, H. Roozekrans et al, "Cloud forecasting for earth observation satellites", BCRS report USP-2, 98-20, 1999

TABLE I. REAL-TIME CONCEPTS

Concept	Characteristics				
	Sensor pointing	*Man-in-the-loop*	*Communication*	*Processing*	*Margin ratio M*
On-board sensor	2D pointable	no	Direct interface	On-board	1.75
µsat at close distance	Fixed nadir	no	Inter-satellite link	On-board	1.49
µsat at larger distance	Fixed nadir	yes	Downlink	On-ground	1.76
µsat with dual sensor	Fixed angles	yes	Downlink	On-ground	1

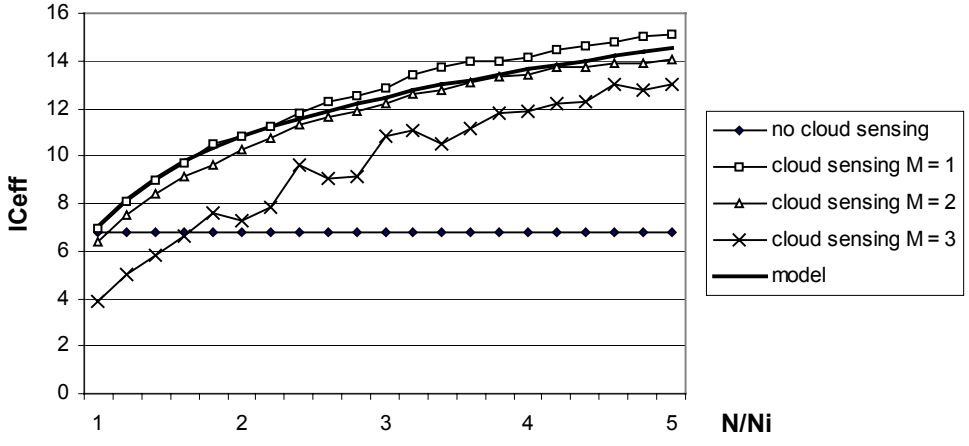

Figure 1. Simulation results: effective imaging capacity (number of cloud-free images per pass) with and without cloud sensing for a 500x500km area in Western Europe as a function of the ratio of N and N_I .